

UNIVERSITY OF CALIFORNIA - BERKELEY

TWO-WEEK LOAN COPY

*This is a Library Circulating Copy
which may be borrowed for two weeks.
For a personal retention copy, call
Tech. Info. Division, Ext. 5545*

RADIATION LABORATORY

DISCLAIMER

This document was prepared as an account of work sponsored by the United States Government. While this document is believed to contain correct information, neither the United States Government nor any agency thereof, nor the Regents of the University of California, nor any of their employees, makes any warranty, express or implied, or assumes any legal responsibility for the accuracy, completeness, or usefulness of any information, apparatus, product, or process disclosed, or represents that its use would not infringe privately owned rights. Reference herein to any specific commercial product, process, or service by its trade name, trademark, manufacturer, or otherwise, does not necessarily constitute or imply its endorsement, recommendation, or favoring by the United States Government or any agency thereof, or the Regents of the University of California. The views and opinions of authors expressed herein do not necessarily state or reflect those of the United States Government or any agency thereof or the Regents of the University of California.

UCRL-1575
Unclassified-Chemistry Distribution

UNCLASSIFIED

UNIVERSITY OF CALIFORNIA

Radiation Laboratory

Contract No. W-7405-eng-48

THE SELF-SCATTERING AND SELF-ABSORPTION OF BETA PARTICLES BY MODERATELY
THICK SAMPLES

W. E. Nervik and P. C. Stevenson

November 21, 1951

Berkeley, California

THE SELF-SCATTERING AND SELF-ABSORPTION OF BETA PARTICLES BY MODERATELY THICK SAMPLES

W. E. Nervik and P. C. Stevenson

Radiation Laboratory and Department of Chemistry
University of California, Berkeley, California

November 21, 1951

ABSTRACT

A study has been made of the effect of moderately thick samples (1-20 mg/cm²) on the observed counting rate of beta active isotopes. Homogeneous mixtures of inactive salt [NaCl or Pb(NO₃)₂] and carrier-free active material having a single component beta spectrum were mounted in uniform deposits on steel plates, and the counting rate observed as the thickness of inactive salt was varied between 1 and 20 mg/cm². The effect has been measured for six active isotopes having maximum beta energies between 0.167 and 2.2 Mev. When compared to the counting rate of carrier-free active material, all thick samples except the 0.167 Mev beta in NaCl show an initial rise in the observed counting rate, followed by a gradual decrease as the sample thickness increased. This is interpreted to mean that scattering of beta particles into the Geiger counter is the preferential process at low sample thicknesses and that absorption of beta particles by the sample gradually becomes more important as the sample thickness is increased.

THE SELF-SCATTERING AND SELF-ABSORPTION OF BETA PARTICLES BY MODERATELY THICK SAMPLES

W. E. Nervik and P. C. Stevenson

Radiation Laboratory and Department of Chemistry
University of California, Berkeley, California

November 21, 1951

INTRODUCTION

In the spallation and fission yield studies in the Chemistry Division of the University of California Radiation Laboratory at Berkeley the problem of the effect of finite sample thicknesses on the observed counting rates of active materials has long been a perplexing one. In order to get absolute cross sections, samples containing inactive carriers are prepared which usually have a thickness between 1 and 20 mg/cm². Since no systematic data showing the effect of samples of this thickness on the observed counting rates have been available, corrections for self-scattering and self-absorption could not be made with any degree of certainty. Corrections of this type are essential, however, if absolute disintegration rates of any reliability are to be obtained. It was felt, therefore, that an investigation of the self-scattering and self-absorption phenomenon in salts having a wide variation in atomic number and with active isotopes having a broad spread of beta energies would be most profitable.

PROCEDURE

In order to get data which were consistent over a wide range of beta energies, it was considered desirable that a single inactive salt be used as the self-scattering and self-absorbing medium in the sample. With this in mind, the problem was essentially one of getting a uniform, homogeneous deposit of salt containing a known amount of carrier-free active material mounted in a known area. The procedure used for obtaining this deposit should be such that successive layers of the same composition could be placed over the same area in approximately 1 mg/cm^2 increments so that counts could be taken, and the self-scattering and self-absorption effects measured, at each increment.

As finally developed, the technique of preparing the samples and measuring the self-scattering and self-absorption factor (hereafter called F_{ssa}) was as follows:

1. An aliquot (usually about 20,000 counts per minute) of solution containing the carrier-free active material was placed on a very thin (approximately $5 \text{ } \mu\text{g/cm}^2$) zapon film, evaporated to dryness, and counted.*

* All counts used to obtain the self-scattering and self-absorption data were taken on shelf 2 (2.04 cm shelf to window distance) of the Geiger counter sample holder of Fig. 1, using an argon-chlorine filled Amperex 100 C tube. In order to check any variation in the self-scattering and self-absorption effect at other sample to window distances, several runs were made in which the sample was mounted on shelf 5 (6.81 cm shelf-to-window distance). No difference between the F_{ssa} values on shelf 5 and those on shelf 2 were noticed which exceeded the experimental error (values for the two shelves checked to within $\pm 2\%$).

This gave an initial count, C cpm/ μ l, for the solution. It was assumed that there was no backscattering of beta particles from the Zapon film and no self-scattering or self-absorption by the carrier free sample itself.

2. Stainless steel filters approximately 1.5 cm in diameter and 3 mm thick were obtained from the Micro Metallic Corporation of Brooklyn, New York.* This thickness is sufficient to give "saturation backscattering" with all beta energies used. These filters were washed repeatedly with 1 N HNO_3 and distilled H_2O , dried at $1300C$, and weighed. The washing, drying, and weighings were repeated until three successive weights agreed to ± 0.02 mg, after which the filter was placed in the dust collecting apparatus (described in step 3) and "filled" with approximately 1 mg/ cm^2 of inert NaCl. The "filled" plates were then mounted directly below the Zapon film of step 1, as close as possible to the film without touching it, and a second count taken. This gave

* The manufacturer claims that filters of this type will stop dust particles whose diameters are greater than two microns. In preliminary experiments with the dust collecting apparatus a slight penetration of the untreated plates by active dust was noticed, probably due to a relatively low number of excessively large pores in the surface of the filter. When the plates were "filled" with a deposit of NaCl approximately 1 mg/ cm^2 thick, penetration was not detectable either by anomalies in subsequent data or by physically milling off a thin layer of the steel filter. It was assumed, therefore, that all deposits collected on the NaCl "filled" plates were on the surface and that there was no penetration of active material into the body of the filter.

a count C_0 which was higher than C because of backscattering of beta particles by the steel plate, i.e., $C_0 = F_b C_{cpm/\mu l}$ where F_b is the back-scattering factor (1, 2, 3).

3. A solution was made up of a precisely weighed amount of inert salt [NaCl or $Pb(NO_3)_2$] and an aliquot (usually about 150,000 cpm) of the solution used in step 1. This solution, after thorough mixing, was placed in the aspirator unit of the "dust" making apparatus of Fig. 2. The steel filter of step 2, washed to constant weight, filled with NaCl, and measured for back-scattering, was placed in the plate holder unit inside the radiant heater of Fig. 2. An exploded view of the plate holder unit is shown in Fig. 3 for clarity. Three white Teflon gaskets were used in the unit; one below the steel filter to form a tight seal with the lower brass fitting, one above the filter to form a seal with the upper brass fitting and to define the area over which the dust could be collected on the upper surface of the filter, and a third one to form a seal between the upper brass unit and the glass of the heating chamber of Fig. 2. When assembled, the three bolts, fitted into slots in the brass fittings, were tightened and the steel filter was held rigidly in position between the Teflon gaskets. Two Variacs, controlling current to nichrome coils surrounding the heating chamber and the radiant heater of Fig. 2, were turned on and enough time was allowed for the internal temperature of the heating chamber and plate holder unit to reach approximately 130° C. Then a Megavac pump, connected to the lower end of the plate holder unit, and positive air pressure, connected to the inlet tube of the aspirator unit, were turned on. Under normal running conditions there was a positive

pressure of approximately 10 in. mercury on the air inlet side of the aspirator, a negative pressure of approximately 5 in. mercury inside the aspirator and heating chamber, and a negative pressure of approximately 27 in. mercury on the vacuum pump side of the steel filter. This pressure sequence caused the solution in the aspirator to be drawn through the aspirator nozzle and ejected as a mist. The largest droplets were not carried by the air stream, and merely returned to the main body of solution, while the finest droplets were drawn into the heating chamber. Here, where the temperature was kept at approximately 130° C, the water was completely evaporated, leaving a residue of "dust" particles. The particles and steam formed in the heating chamber were then drawn down to the filter, where the particles were collected and the steam passed through. When the apparatus had been run long enough for approximately 1 mg/cm² to have been collected, the steel filter was removed, cooled to room temperature in a dessicator, weighed, and counted. Now the assumption was made that droplets ejected by the aspirator would have the same concentration of salt and active material as the parent solution. If this be true, then the specific activity of the "dust" particles should be known, since the ratio of isotope activity to weight of salt was known when the parent solution was made up. Therefore, if the salt had no self-scattering or self-absorbing effect on the beta activity, the specific activity of the particle is

$$C_1 = \frac{\text{number of cpm of activity added}}{\text{mg salt used}} = \frac{(C_0 \frac{\text{cpm}}{\mu\text{l}})(\mu\text{l used})}{\text{mg salt}} \quad (\text{from step 2}).$$

From the weight of salt collected and the number of counts observed on an individual sample, a specific activity C_{obs} (counts/mg) could be computed,

and the ratio of C_{obs} to C_1 would give the self-scattering and self-absorption correction factor for this beta energy and thickness of salt, i.e.,

$C_{\text{obs}} = F_{\text{ssa}}(C_1)$. This process of mounting in the apparatus, depositing a thin layer of salt, cooling, weighing, counting, and computing F_{ssa} was continued with the same plate until a layer of approximately 20 mg/cm^2 had been built up. Salt deposits collected in this manner (a sample of which is shown in Fig. 4) usually were in the form of a very hard cake evenly distributed over a fixed area, and with quite sharply defined edges. In order to minimize errors due to weighing, counting, or slightly uneven deposits, two separate plates were run on each salt and beta energy combination, and an average taken of the data obtained.

RESULTS

Correction factor (F_{ssa}) vs. sample thickness curves were obtained for each of the carrier-free isotopes mixed with known amounts of NaCl and $\text{Pb}(\text{NO}_3)_2$. These salts were selected because they seemed to meet the necessary requirements for solubility and temperature stability needed in the atomizer and deposit collecting apparatus. Six active isotopes were used in the experiments, pertinent data for which are summarized in Table I.

Table I

Salts and Beta-Active Isotopes Used for Measuring
Self-Scattering and Self-Absorption

Isotope	Half-Life	Maximum Beta Energy (Mev)	Salts for which Data were Obtained
S^{35}	87 d	0.167	NaCl, $\text{Pb}(\text{NO}_3)_2$
Pm^{147}	4 y	0.223	NaCl, $\text{Pb}(\text{NO}_3)_2$
W^{185}	73 d	0.43	NaCl
Pr^{143}	13.8 d	0.92	NaCl, $\text{Pb}(\text{NO}_3)_2$
P^{32}	14.3 d	1.7	NaCl, $\text{Tl}(\text{NO}_3)_2$
Y^{90}	65 h	2.2	NaCl, $\text{Pb}(\text{NO}_3)_2$

On the P^{32} - $Pb(NO_3)_2$ run it was noticed that the P-Pb compound [presumably $Pb_3(PO_4)_2$] had a marked tendency to stick to the glass walls of the aspirator unit. $Tl(NO_3)_3$ did not behave in this manner and was used for the P^{32} run in place of $Pb(NO_3)_2$. In the W^{185} run, both $Pb(WO_4)$ and $Tl_2(WO_4)_3$ formed insoluble precipitates* which prevented collection of a sample which had a known specific activity, therefore no salt which had a high atomic number was used for this beta energy.

Curves of F_{ssa} vs. sample thickness, which were obtained for NaCl and $Pb(NO_3)_2$, are plotted in Figs. 5 and 6. The two individual runs of any salt-beta energy combination are plotted with the same symbol in order to facilitate reading of these charts. In most cases the difference between these runs did not exceed $\pm 3\%$, and there was no question as to where the average curve should be; in those cases where the difference was greater than this, a curve was usually drawn half way between the individual curves.

In order to facilitate interpolation, it was considered desirable that curves be drawn for more even beta energy intervals. To do this,

* The W^{185} solution, which was obtained from the Oak Ridge National Laboratory, contained 14.8 mg/ml W, 44.0 mg/ml total solids, and 38.5 mg/ml non-volatile materials. This amount of W was enough to form a visible precipitate even when diluted 30:1 in the aspirator solution. The remaining five active isotopes were obtained in carrier-free solutions which contained negligible amounts of non-volatile solid material.

data on F_{ssa} vs. beta energy were taken from Figs. 5 and 6 for sample thicknesses of 3, 5, 10, 15 and 20 mg/cm^2 and plotted as in Fig. 7. These data gave points for reasonably smooth curves, from which F_{ssa} vs. sample thickness values were taken for beta energies of 0.15, 0.2, 0.3, 0.4, 0.6, 0.8, 1.0, 1.5, 2.0, 2.5, and 3.0 Mev and plotted in Figs. 8 and 9.

All of the F_{ssa} vs. sample thickness curves, of which those in Fig. 8 are representative, showed the same general characteristics. There was an initial rise in the F_{ssa} factor for relatively thin samples, a leveling off, and then a gradual decrease in the factor as the sample thickness increased. Since scattering and absorption are both affecting the observed counting rate, this can only be interpreted to mean that self-scattering is by far the more important phenomenon in thin samples and that self-absorption does not become critical until the deposit thicknesses approach an appreciable fraction of the half-thickness for beta particles in the salt. Thus, in Fig. 8, the curve for 0.2 Mev shows a maximum F_{ssa} value of 1.02 at a sample thickness of 1 mg/cm^2 . Since the half thickness for 0.2 Mev beta particle is approximately 4 mg/cm^2 (4), absorption is noticeable at 2 mg/cm^2 , and the curve shows predominantly an absorption effect for thicker samples, decreasing continuously to a value of 0.41 at 20 mg/cm^2 . The curve for 1.5 Mev, however, where the half-thickness is approximately 90 mg/cm^2 , shows a fairly rapid rise at low sample thicknesses, and has apparently just reached its maximum value of 1.16 at 20 mg/cm^2 . Here the sample has not yet reached a thickness at which absorption plays an important part and the scattering effect is still predominant.

After the first few curves were obtained, an attempt was made to find a theoretical equation which would describe the data. The most successful one took the form

$$(a) \quad C_{\text{obs}} = (C_0/\lambda)(1 - e^{-\lambda t})(1 + Be^{-\lambda t})(1 + b(1 - e^{-kt}))$$

where C_{obs} = counts observed

C_0 = counts with zero self-scattering, self-absorption, and backscattering

$\lambda = 0.693/T_{1/2}$, where $T_{1/2}$ is the half-thickness in aluminum for beta particles of this energy (4)

B = backscattering factor for the plate on which the sample is mounted

K and b are parameters, analogous to a backscattering factor and absorption coefficient respectively, for the salt with which the active material is mixed.

Preliminary trials showed that with proper adjustment of the constants b and K curves could be obtained which would follow the experimental data quite satisfactorily between 0 and 20 mg/cm². As a check on the reliability of this equation at higher sample thicknesses, and to find out how the higher energy beta curves would behave in thicker samples, a NaCl-P³² run was made in which the sample thickness was built up to 80 mg/cm². The curve drawn for this run is presented in Fig. 10. Although the curve drawn from equation (a), (where $T_{1/2} = 105$ mg/cm², $B = 0.421$, $b = 0.27$ and $k = 0.19$), follows the data fairly well up to 12 mg/cm², it "turns down" much too soon and gives low values for all thicker samples.

Since all subsequent attempts to fit the data to a theoretical curve failed, it was decided to use the curves in Figs. 8 and 9 empirically

to estimate the self-scattering and self-absorption effect for beta particles in this type of sample. The procedure in use at the present time is as follows:

Samples are mounted on 1 mil aluminum dishes having a depth of approximately 1 mm and an area of 1 cm². The dishes are mounted on aluminum plates which are thick enough to give saturation backscattering for all beta particles observed, backscattering factors for which are obtained from Jaffe and Justus(1) or Burt(2).

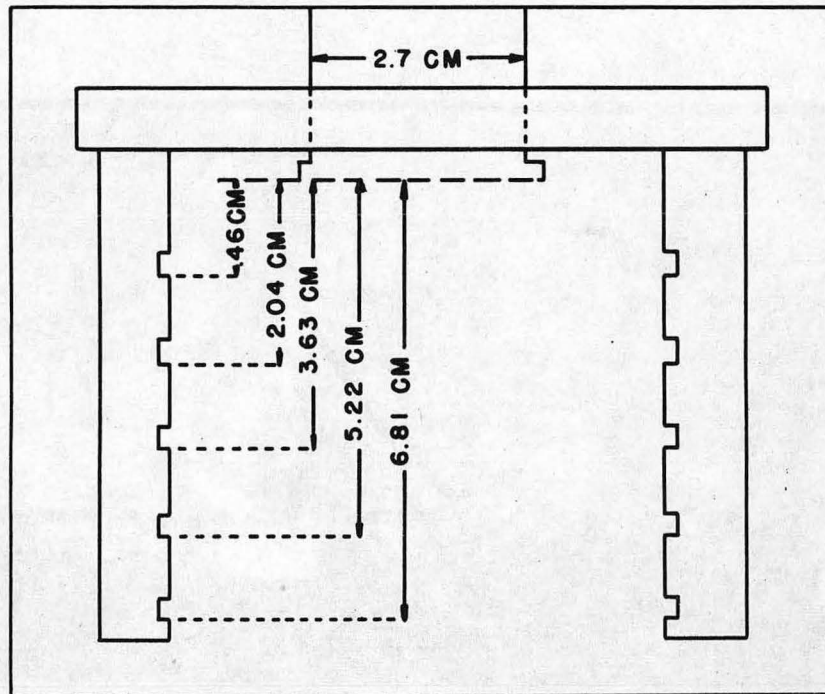
From the known weight of sample and an estimate of the area covered, the sample thickness may be computed. The accuracy of this value, of course, will depend on how evenly the sample is spread in the dish. Using Fig. 8 or 9 with the values for sample thickness, beta energy, and type of salt in which the activity is present, a value of F_{ssa} can be estimated. Since it is obviously impractical to measure F_{ssa} for salts of all atomic numbers, an interpolation is necessary between the values for NaCl and Pb(NO₃)₂. It is not to be expected that data obtained by this type of interpolation will have an accuracy better than $\pm 5\%$, but this should be satisfactory for all but the most precise absolute beta counting.

ACKNOWLEDGMENT

The authors wish to express their gratitude to Dr. E. Nielsen, Mr. M. Thaxter and the members of the Health Chemistry group of the University of California Radiation Laboratory for their aid in developing the apparatus used in these experiments, and to Drs. G. T. Seaborg, I. Perlman, and R. L. Folger for their interest and advice. This work was performed under the auspices of the United States Atomic Energy Commission.

REFERENCES

1. L. Yaffe and K. M. Justus, "Backscattering of Electrons into Geiger-Müller Counters," J. Chem. Soc. (London), Supplement No. 72, S341-351 (1949).
2. B. P. Burtt, Nucleonics, 5, no. 2, 28 (1949).
3. L. R. Zumwalt, U. S. Atomic Energy Commission Declassified Document MDDC-1346 (September 18, 1947).
4. R. Seelmann-Eggebert, Naturwiss. 31, 201 (1943).



MU2909

Fig. 1 Geiger Counter Sample Holder Geometry

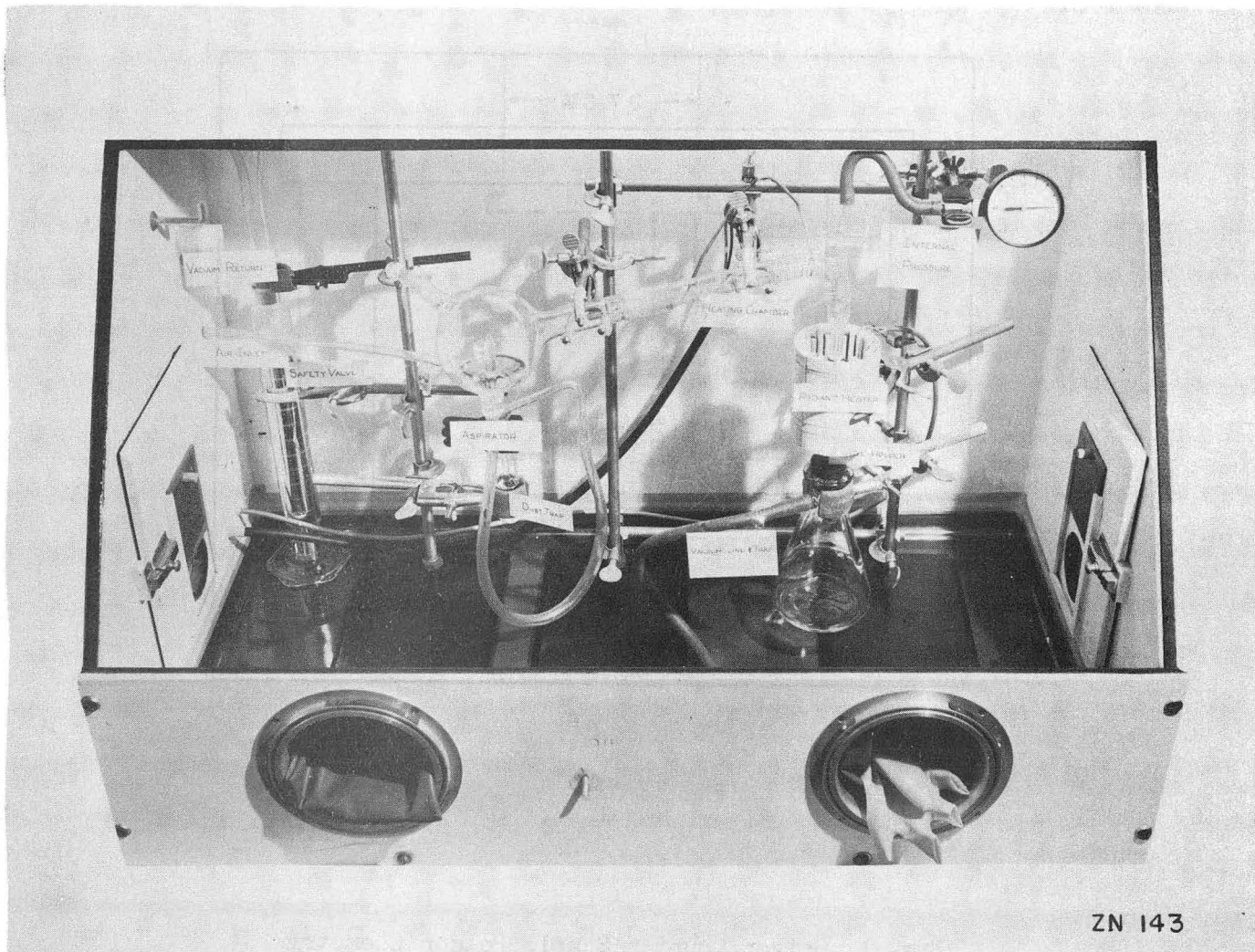


Fig. 2. Dust collecting apparatus used to Prepare samples.

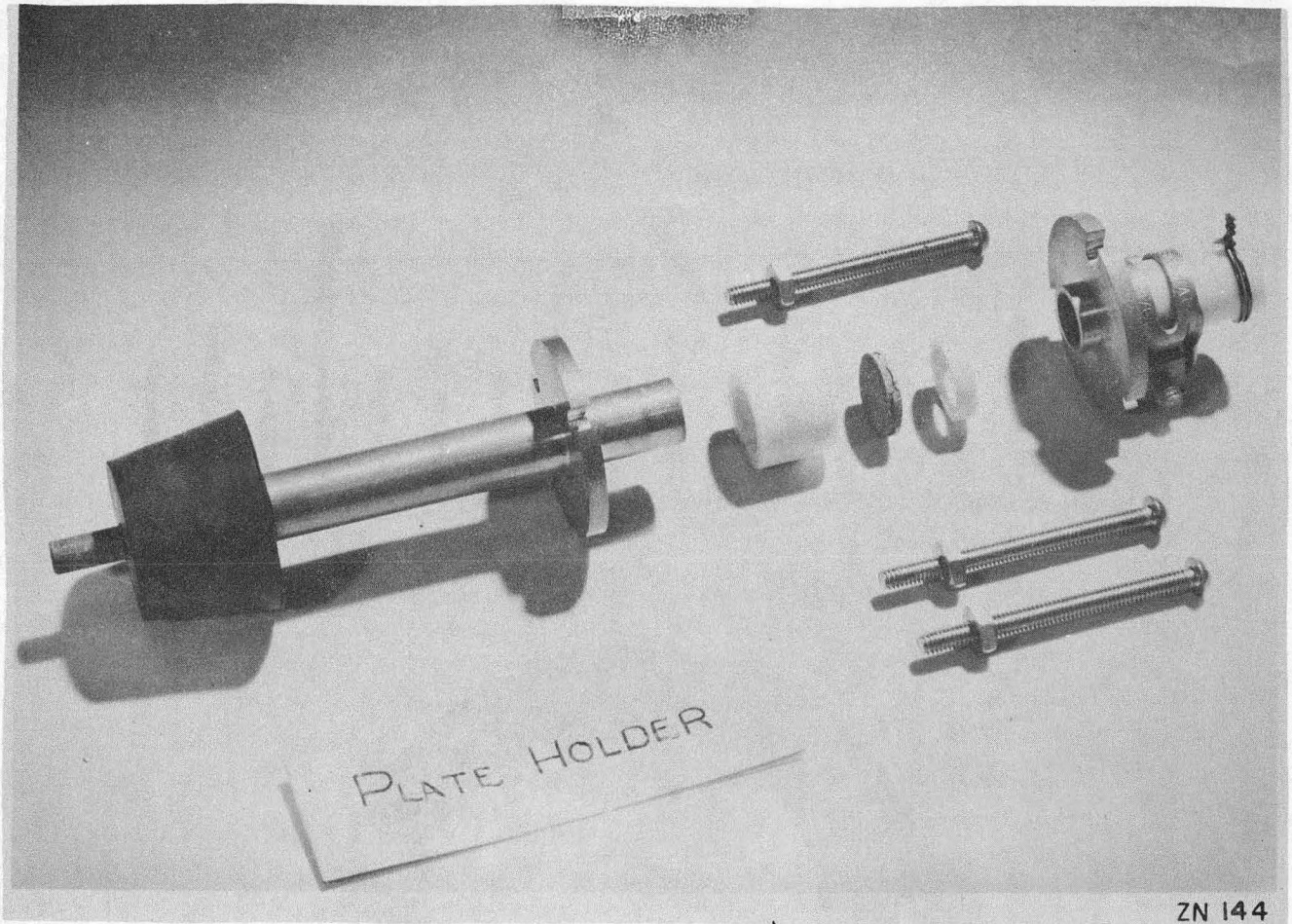


Fig. 3. Plate holder unit of the dust collecting apparatus.

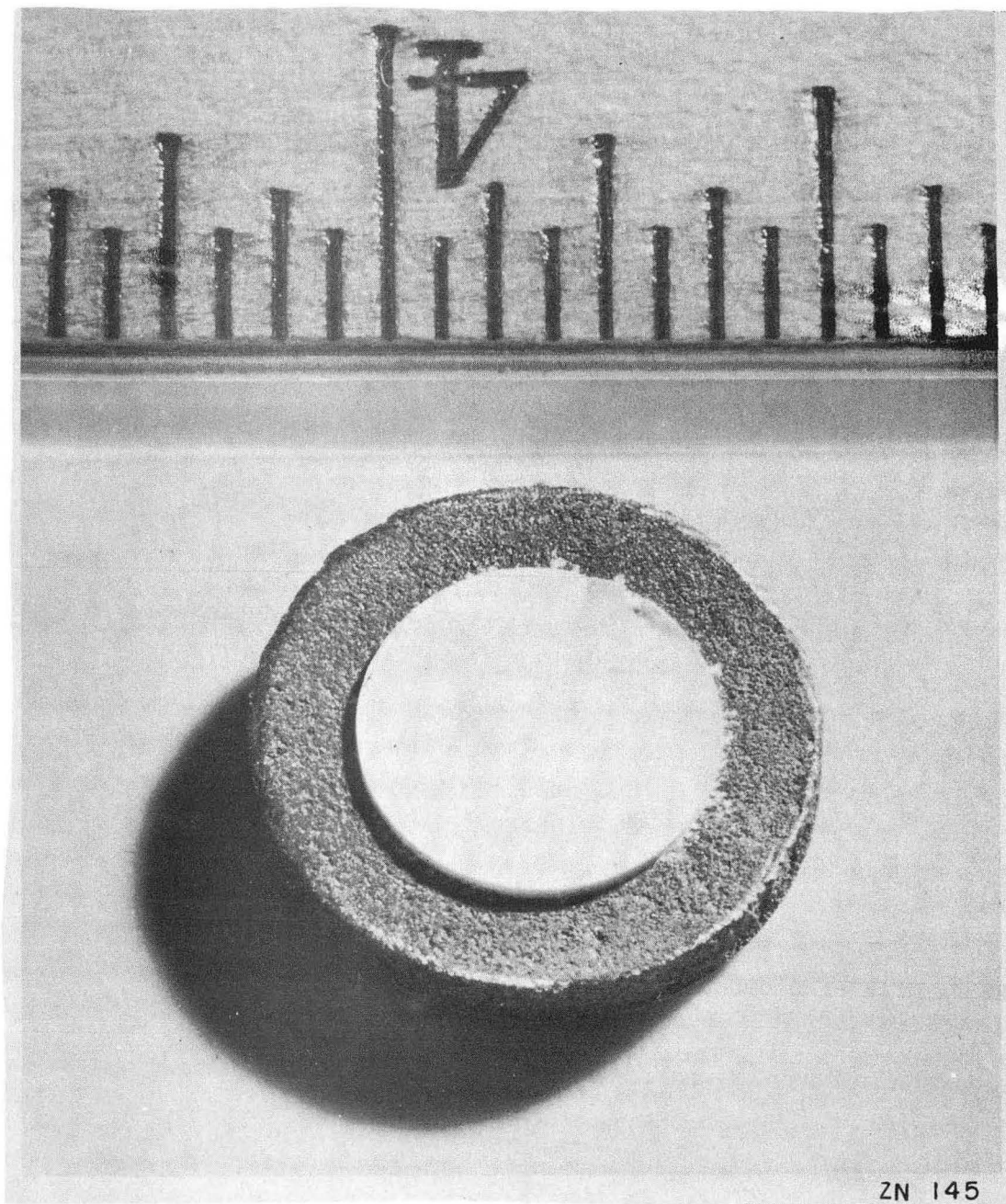


Fig. 4. Sample of $10 \frac{\text{mg}}{\text{cm}^2}$ NaCl prepared in the dust collecting apparatus.

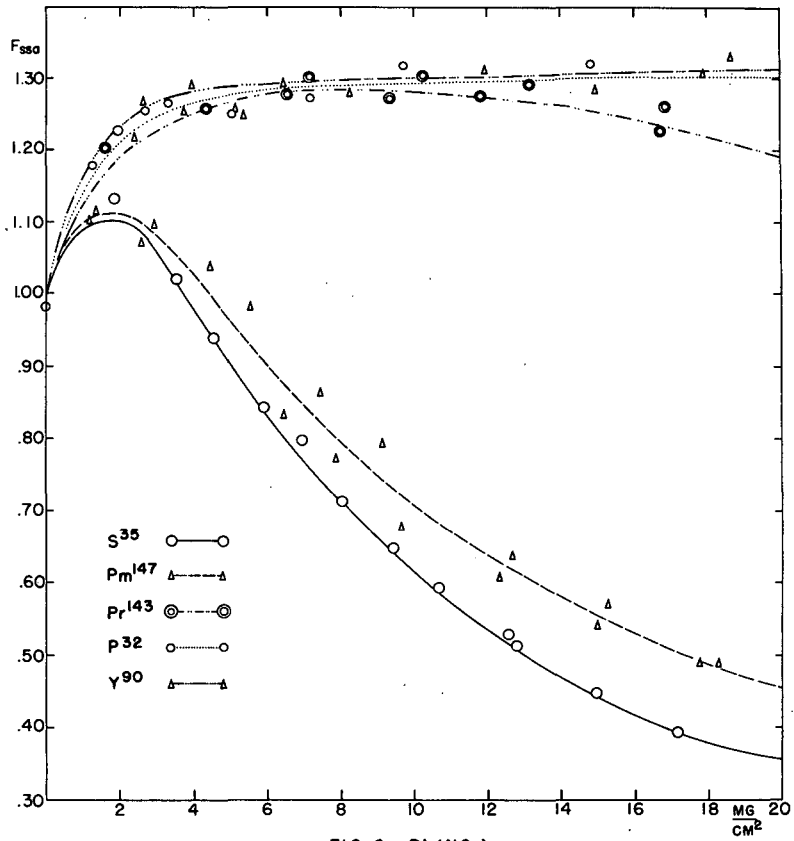


FIG. 6- $Pb(NO_3)_2$

MU 2911

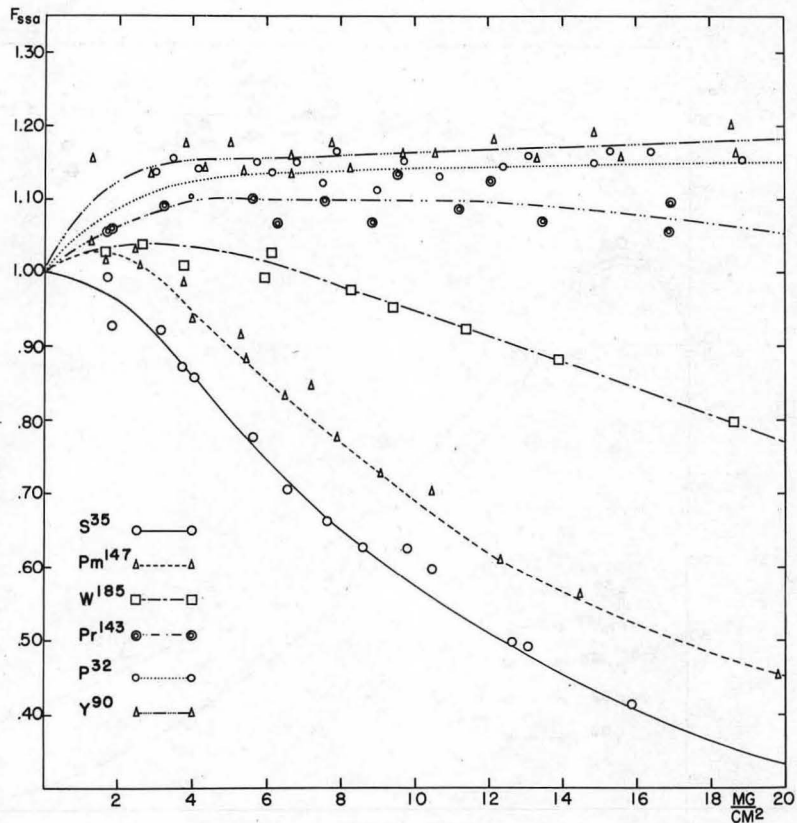


FIG. 5 - NaCl

MU 2910

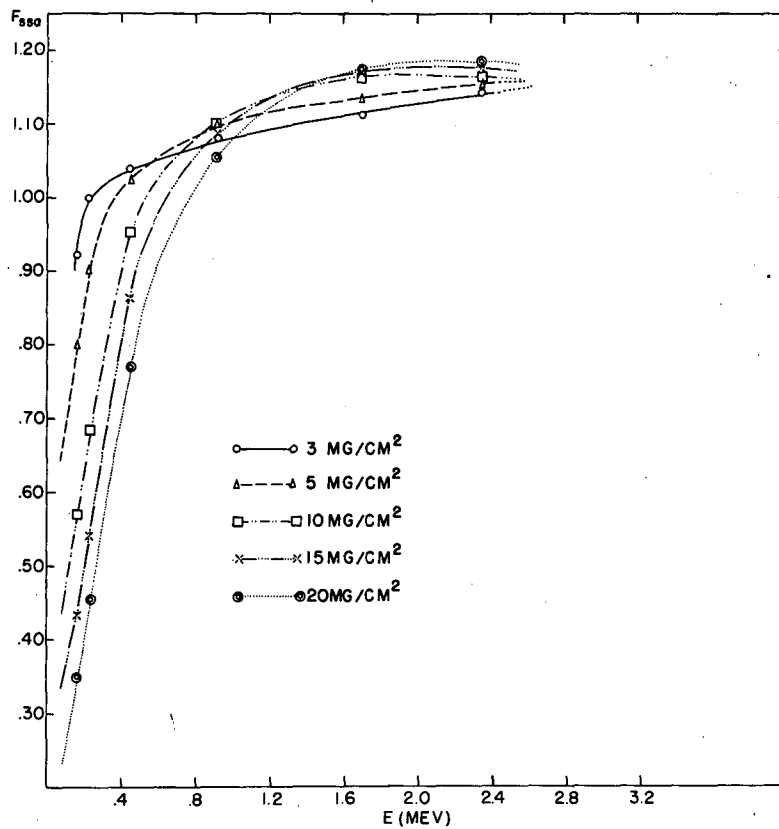
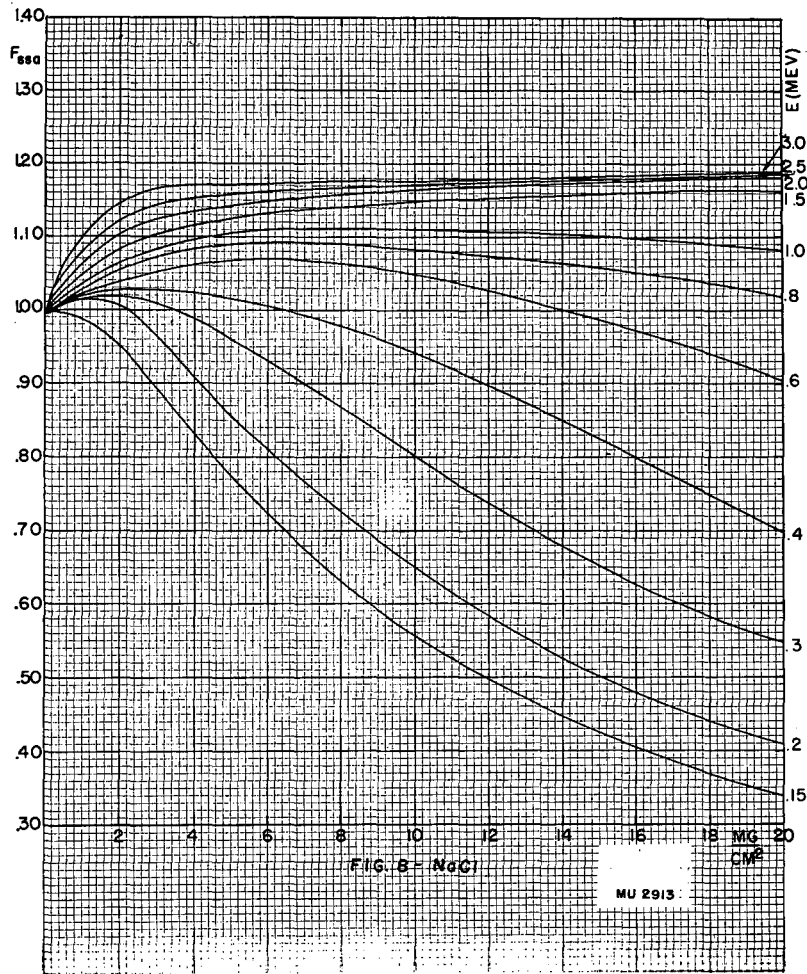


FIG. 7 - $E_{(MAX)}$ VS. F_{880} CURVES FOR NaCl

MU 2912



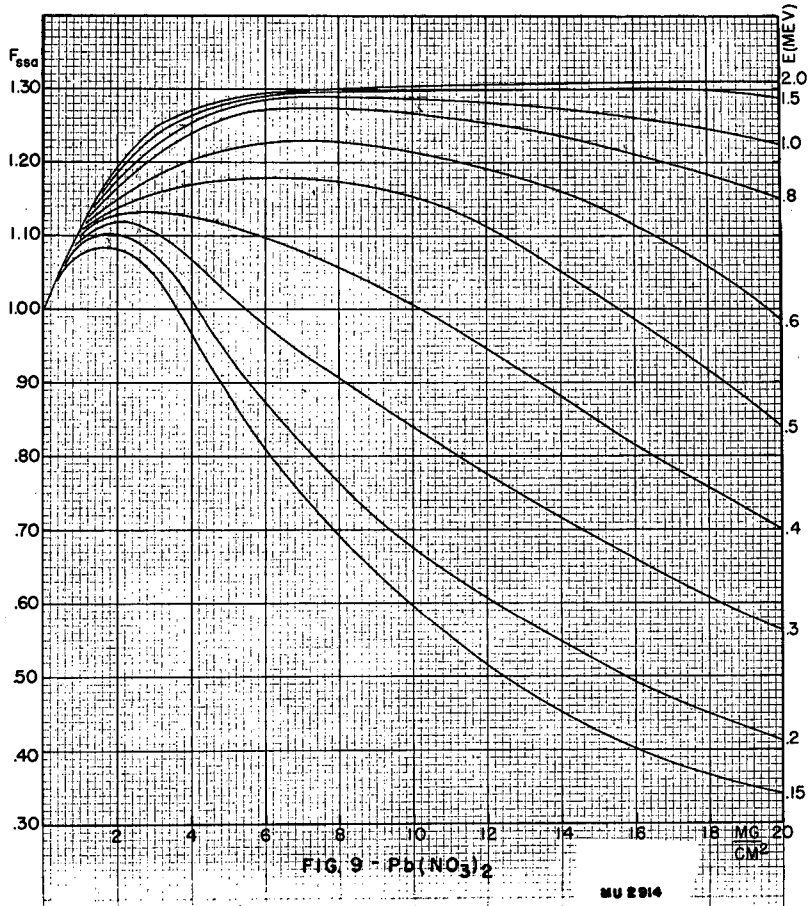


FIG. 9 - $Pb(NO_3)_2$

MU 2314

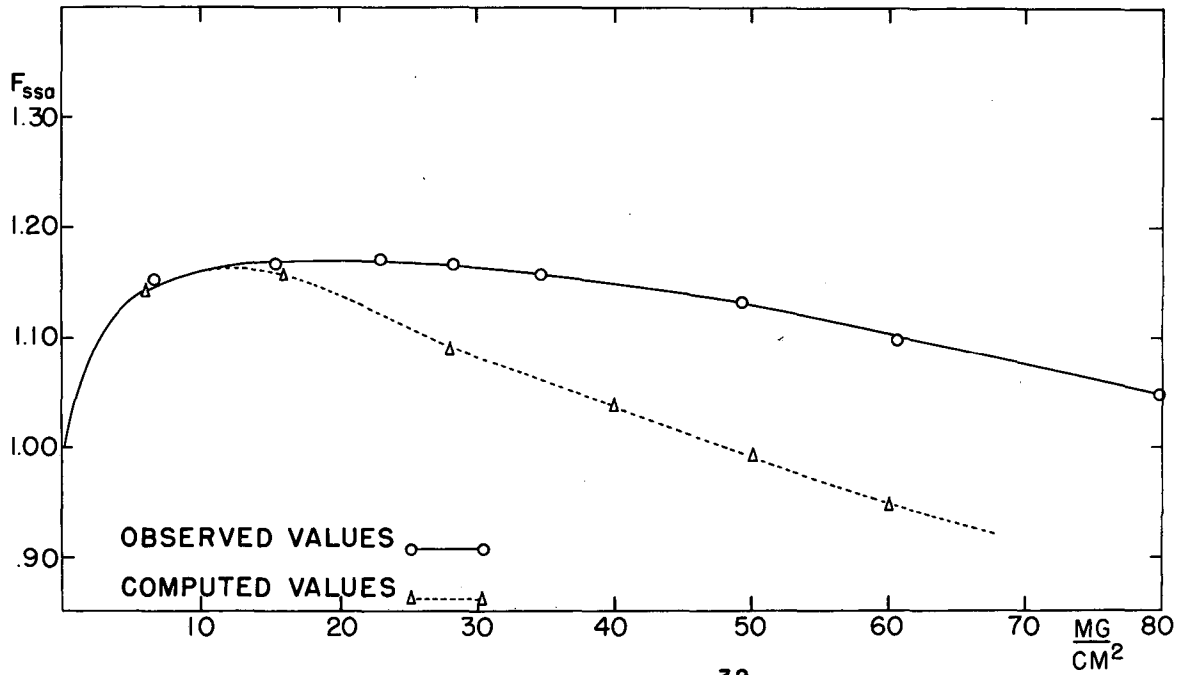


FIG. 10 - NaCl-P³²

MU 2915